Journal of Nuclear Materials 385 (2009) 495–503

Contents lists available at ScienceDirect

Journal of Nuclear Materials

journal homepage: www.elsevier.com/locate/jnucmat

Corrosion resistance of molybdenum-containing titanium alloy for overpack in simulating underground environment

Toshiyasu Nishimura *

National Institute for Materials Science (NIMS), 1-2-1, Sengen, Tsukuba, Ibaraki 305-0047, Japan

ARTICLE INFO

Article history:
Received 4 March 2008
Accepted 1 September 2008

ABSTRACT

Crevice corrosion behavior of titanium (Ti) and binary Ti alloys containing 5–25 mass% of molybdenum (Mo) was investigated in 10% NaCl at 100 °C. Although a considerably large shift in crevice potential toward the active region and large current were observed with Ti, no change in crevice potential or current was observed with the Mo–Ti alloy. The resistance against crevice attack was found to depend on the Mo content of the alloys in the experiment. Further investigations by potentiodynamic polarization and the electrochemical impedance spectroscopy (EIS) method were conducted. Polarization measurements showed an increase in cathodic current density with the increase of Mo content in Ti alloys. As the Mo content was increased to around 10%, the corrosion potential was found to exist within the passive region even in highly acidic solutions. These results illustrated the more highly passivating behavior of 10–25% Mo–Ti alloys than pure Ti and 5% Mo–Ti alloys. The higher impedance values shown by EIS revealed the high ability of 15% and 25% Mo–Ti alloys to keep the passive film even in the acidic solutions. It was found that Mo–Ti alloy could keep the passive film even in a high chloride concentration environment at 100 °C. Hence, as for the crevice corrosion, this alloy could be useful for environments simulating the overpack near the coast.

1. Introduction

It is required that the overpack should be guaranteed the geological disposal of high-level radioactive waste for more than several hundred years. However, candidate materials of overpacks suffer from corrosion due to surrounding groundwater. The corrosion of metals depends mainly on the chemical composition of groundwater, and in Japan, there is a high possibility of the presence of high-concentration chloride solution from the sea. Moreover, the temperature at the surface of the overpack may be as high as 100 °C due to radioactive waste. Ti alloy is a candidate material for such corrosive conditions. While extensive studies have been carried out on the corrosion behavior of Ti, very little information is available on the crevice corrosion in environments simulating the overpack under the ground near the coast. In general, the excellent corrosion resistance offered by Ti is directly related to the formation of a stable surface oxide film of TiO_2. However, Ti is susceptible to crevice corrosion when exposed to environments containing a high-concentration of chloride at elevated temperatures [1–6]. Much effort has been made to improve the stability of the surface film of Ti by suitable alloying [7–15]. Although Pd–Ti alloy was developed and could have high resistance against crevice corrosion at 100 °C, Pd is very rare and expensive. Instead of Pd–Ti alloy, we have been interested in Mo–Ti alloy, however, there have been few investigations of its crevice corrosion. On the other hand, it is important to understand the mechanism of crevice corrosion of Ti alloys. Hence, in the present work, the changes in chloride ion concentration, pH and potential within the crevice were monitored for long periods of exposure by using microelectrodes. The results of these measurements and the results obtained from polarization and EIS techniques were compared to understand the crevice corrosion resistance of 15% Mo–Ti alloy.

2. Experimental method

Ti alloys containing 5–25 mass% of Mo in the base metal of pure Ti (ASTM Grade-2) were made in the present investigation. The ingots of the size in 60 × 150 × 15 mm were melted by arc-melt process using pure Mo and Ti (Grade-2). Then, they were subjected to the solution heat-treatment at 900 °C for 1 h and water quench. It was found that there was no crack in the ingot by X-ray examination. Moreover, the chemical compositions of the several part of the ingot were checked, and there was little segregation all over the ingot. The test specimens were cut by wire-cutting process to prevent the clacks.

The pH microelectrode was fabricated from 0.3 mm diameter tungsten (W) wire, which was partially sealed in a capillary tube. The W wire was then oxidized in 10% nitric acid solution for 18 h

* Tel.: +81 29 859 2127; fax: +81 29 859 2101.
E-mail address: nishimura.toshiyau@nims.go.jp

0022-3115/$ - see front matter © 2008 Published by Elsevier B.V.
doi:10.1016/j.jnucmat.2008.09.045

to form the W/WOx microelectrode. The chloride ion selective microelectrodes of Ag/AgCl were made from 0.3 mm silver wire partially sealed in a capillary tube, and were electrolyzed in 0.1 M HC1 solution under the potential of 500 mV for 12 h.

As shown in Fig. 1, the working electrodes of $2 \times 2 \times 0.2$ cm for Ti and alloy were covered in a Teflon shim of 0.1 mm thickness and tightly screwed on an acrylic board to make the crevice cell. The counter m from the working one. Three capillary holes of 1 mm diameter were made over the acrylic board to insert the microelectrodes such as Ag/AgCl, W/WOx and micro-SSE. The crevice monitoring was conducted in 10% NaCl with open air condition at 100 °C. Just before the measurement, the surface of the test sample was polished by the 600 paper. The current in the crevice was measured using a zero resistance ammeter. Moreover, the potential inside the crevice was measured by using the micro-SSE. The chloride ion concentration and pH were determined from their corresponding potential −log [C1-] and potential −pH calibration curves. The specimens of pure Ti and Mo–Ti alloy were cut into $1 \times 1 \times 0.2$ cm for the polarization and EIS (Electrochemical Impedance Spectroscopy) studies. These studies were conducted in simulated crevice solution that was 20% NaCl solution adjusted to different pH values at 100 °C. The polarization behavior was measured at the scan rate of 1 mV/s. A frequency response analyzer (FRA) was used for EIS measurements and experiments were conducted with an amplitude of 10 mV and the frequency range from 10 kHz to 3 mHz. Impedance spectra were obtained with specimens in the open circuit (OCP) condition and in the passive region of 500 mV. The breakdown behavior of passive film was observed by EIS using the specimens kept at OCP up to 24 h after setting at 500 mV (passive region) for 1 h.

3. Results and discussion

3.1. Monitoring of crevice corrosion for Ti and Mo–Ti alloy

Fig. 2(a) shows the results of changes in crevice current, and the potential inside and outside the crevice in pure Ti (ASTM Grade-2) and 15% Mo–Ti alloy in neutral 10% NaCl at 100 °C. There was no significant change in crevice current for both Ti and 15% Mo–Ti alloy up to 96 h of monitoring, and then the crevice current of Ti increased suddenly to higher values. At the same time simultaneous

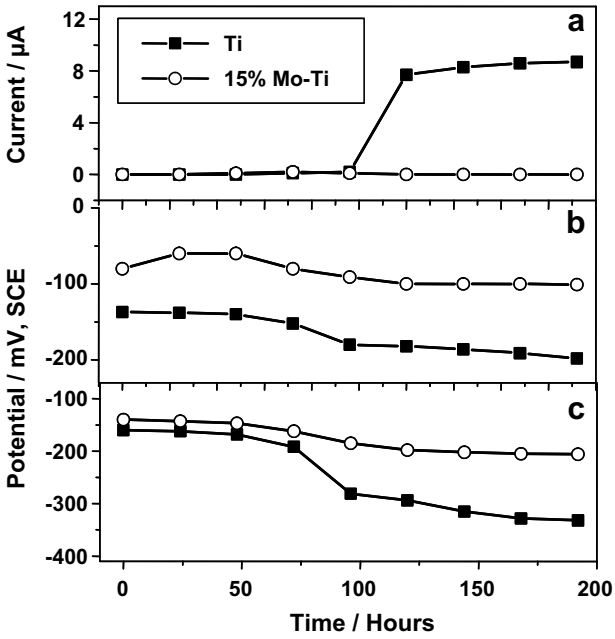

Fig. 2. Changes in (a) crevice current, (b) potential outside crevice and (c) potential inside crevice at 100 °C.

change of potential outside and inside the crevice of Ti from −130 mV to −196 mV and −165 mV to −306 mV, respectively, were observed as shown in Fig. 2(b) and (c). These changes in potential to the more active region reflected the decrease in stability of passive film over the Ti surface and led to active dissolution reaction 1, 3–4) within the crevice. The potential inside the crevice was more sharply detected by micro-SSE than that outside of the crevice. The absence of changes in the above parameters for 15% Mo–Ti alloy suggested that the passive film of the alloy remained stable in this test.

Fig. 3 shows the changes in pH and chloride ion concentration inside the crevice of pure Ti and alloy in 10% NaCl at 100 °C. An increase in chloride ion concentration increased from 10% to 17% at 96 h within the crevice. It is thought that in order to maintain elec-

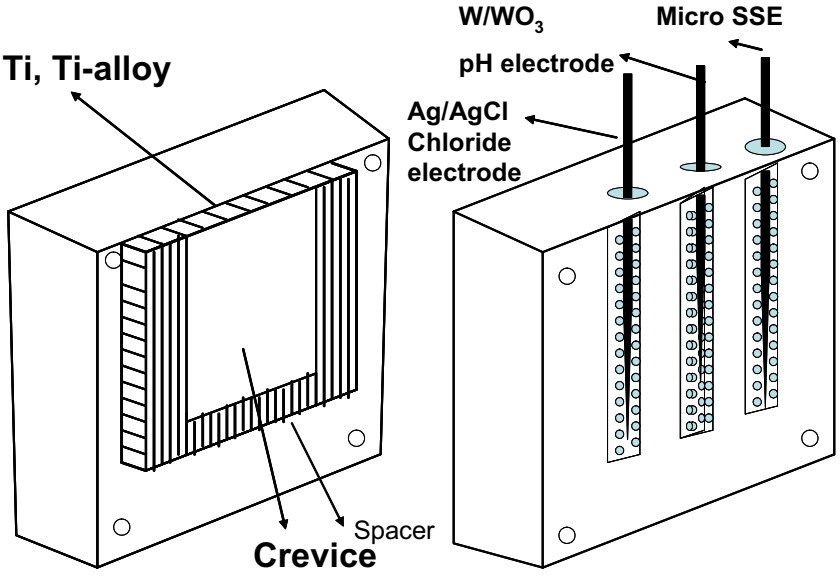

Fig. 1. Schematic diagram of crevice cell using micro electrodes for monitoring.

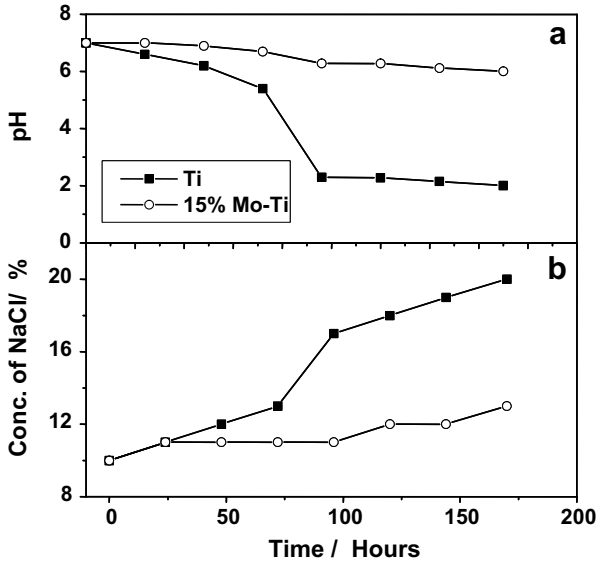

Fig. 3. Changes within the crevice of (a) pH and (b) chloride concentration at 100 °C.

tro neutrality within the crevice, chloride ions migrate from the bulk to the crevice. The pH within the crevice slowly shifted toward lower values and reached a value of pH 2.3 after 96 h for Ti, indicating the predominant dissolution reaction was operating within the crevice. This process produced Ti ions, and the subsequent hydrolysis reaction produced hydrogen ions and further reduced the pH.

The change in solution chemistry observed in the crevice by the combination of increased acidity and higher chloride concentration might result in the continuous propagation of crevice corrosion on pure Ti after 96 h. These phenomena corresponded to the shift of crevice potential from the passive to active region and the increase in crevice current. However, only marginal changes were observed in the above parameters for the Mo–Ti alloy. This behavior of alloy suggested that adding Mo effectively kept the passive film stable even in the high chloride and high temperature condition. In this way, Mo–Ti alloy had no susceptibility to crevice corrosion at the high temperature of 100 °C.

The variation in crevice potential with immersion time for Ti and Mo–Ti alloys containing 5–25 mass% of Mo in pH 4.0 solution of 10% NaCl at 100 °C is shown in Fig. 4. The potential of the creviced Ti was found to change gradually from an initial −360 mV to nobler potential, reflecting the formation of the surface film. After 180 h, the potential was found to change rapidly toward the active region of around −510 mV and then stayed at the same potential up to 500 h of monitoring. This behavior demonstrated the continuous active dissolution reaction taking place within the crevices of Ti, and the susceptibility of pure Ti to crevice attack. A similar trend was observed with 5% Mo alloy as evident from the final crevice potential of around −370 mV. Alloys containing 15% and 25% Mo showed a gradual shifting of crevice potential toward more positive values and reached +6 mV and +30 mV, respectively at the end of 500 h. The positive crevice potential with these alloys suggested the presence of a stable passive film over the surface, which imparted higher resistance against crevice corrosion.

3.2. OCP measurement under simulated crevice solution

To investigate the effect of different Mo alloying content on the passivation of Ti at various acidic conditions in environments of higher chloride concentration, open circuit potential (OCP) was monitored in 20% NaCl at different pH values (Fig. 5). At pH 4.0 solution Ti exhibited an OCP value of −420 mV which shifted to less noble values with a decrease in pH. Thus, Ti was thought to be highly susceptible to crevice corrosion under pH 4.0 solution of 20% NaCl. These observations were in agreement with the results shown in Fig. 4. It was understood that the increase of Cl ions and decrease of pH proceeded in the crevice, and once the pH fell below 4.0, then active corrosion occurred for pure Ti. A similar trend was observed with alloys containing 5% Mo. In the case of 10% Mo–Ti alloy, the pH fell below 2.0, then active corrosion occurred. On the other hand, a quite different behavior was observed for 15% and 25% Mo–Ti alloys. These alloys showed an OCP value of −210 mV and −198 mV respectively in pH 0.5 solution. This observation clearly revealed the existence of the passive condition, which was responsible for providing immunity against crevice corrosion in 20% NaCl. In this way, Mo was shown to be effective against corrosion in acidic solution simulating the crevice at high temperature.

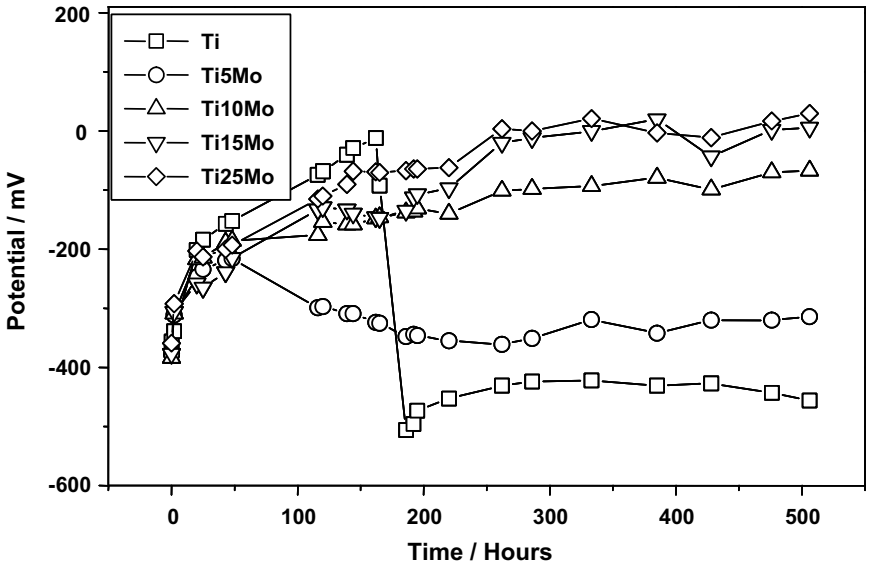

Fig. 4. Change in crevice potential as a function of time for Ti and Mo–Ti alloys in neutral solution of 10% NaCl at l00 °C.

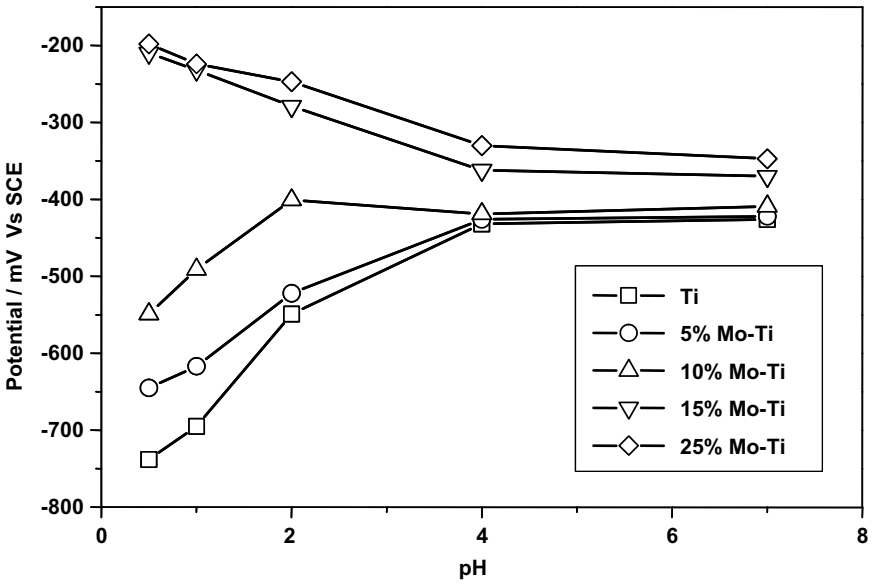

Fig. 5. Open circuit potentials of Ti and Mo–Ti alloys after 1 h immersion in 20% NaCl at 100 °C.

3.3. Potentiodynamic polarization measurements

The polarization behaviors of Ti and Mo–Ti alloys were measured in simulated crevice solution of 20% NaCl at pH 0.5 as shown in Fig. 6. Higher cathodic currents were observed for all Mo–Ti alloys than that of pure Ti. As against the active peak current of 9.8×10^{-4} mA cm^{-2} obtained with pure Ti, there were no apparent active peaks with the alloys in pH 0.5 solution. The higher cathodic currents and lower active peak contributed to ennobling of the corrosion potential (E_{corr}) of Mo–Ti alloys. The E_{corr} values were very high with 15% and 25% Mo–Ti alloys, and existed completely within the passive region around −200 mV. Similar results were obtained with Ti and its alloys in pH 1.0 solution of 20% NaCl at 100 °C. The polarization behavior suggested that the addition of 15% and 25% Mo was effective for maintaining the passive film even in highly acidic crevice environments at elevated temperature. However, the passive current densities of Mo–Ti alloys were slightly higher than that of pure Ti. This might be due to the transpassive dissolution of Mo through the passive film. In this way, it was shown that the ennobling of corrosion potential and maintenance of the passive condition resulted in the higher resistance of 15% and 25% Mo–Ti alloys against crevice corrosion.

3.4. EIS investigation

To confirm the influence of Mo alloying on the resistance of the passive film against crevice attack, EIS measurements were carried out for Ti and Ti alloys in the OCP condition at different pH values of 20% NaCl at 100 °C. From the EIS spectra (Fig. 7), resistance (R_t) values at 3 mHz are plotted in Fig. 8. The pure Ti exhibited a very low value of R_t in the low frequency region in pH 0.5 and 1.0 solution. The phase shift spectra observed for Ti in pH 0.5 and 1.0 solutions suggested the presence of two capacitances; the capacitance at high frequency was thought to be the passive film capacitance. As the lower value of R_t in the low frequency region suggested that the pure Ti underwent active dissolution at these pH values, the

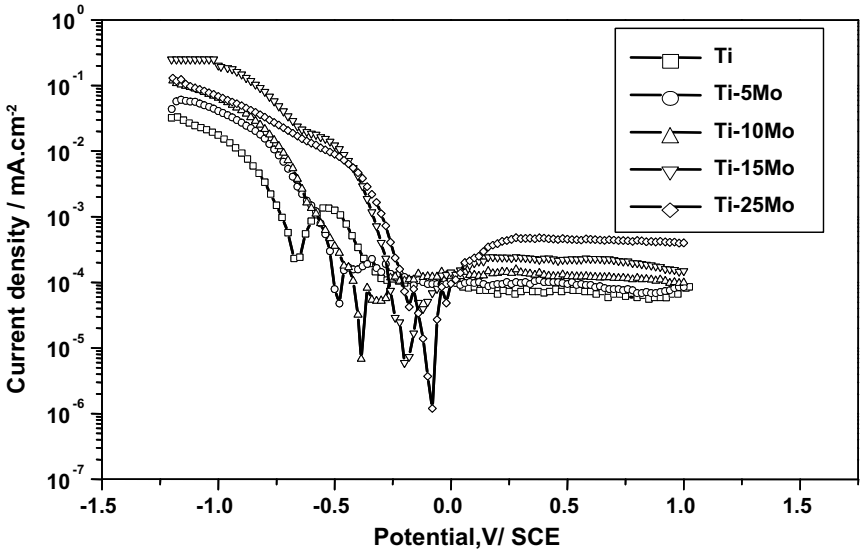

Fig. 6. Polarization behavior of Ti and Mo–Ti alloys in pH 0.5 solution of 20% NaCl at 100 °C.

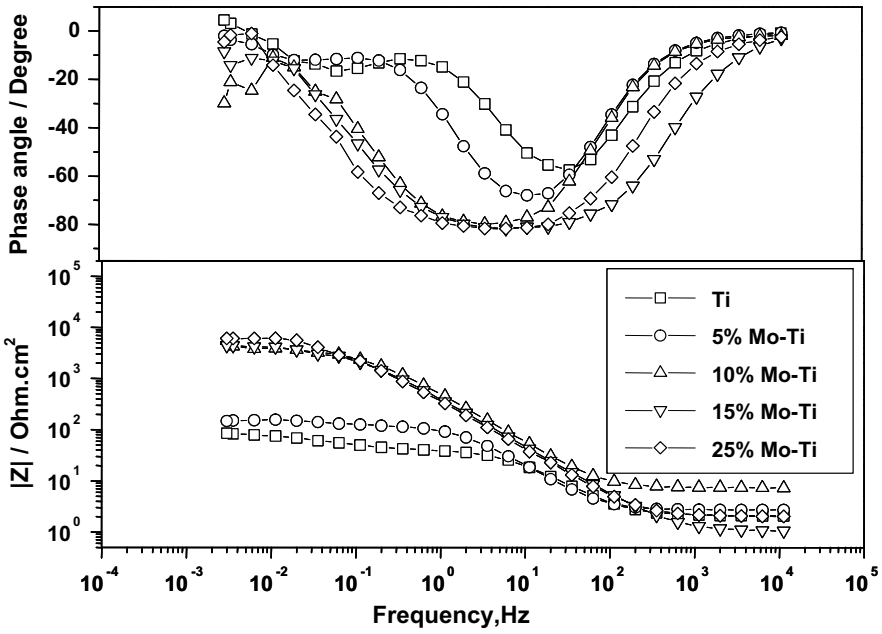

Fig. 7. Impedance behaviors of Ti and Mo–Ti alloys in pH 0.5 solution of 20% NaCl at 100 °C.

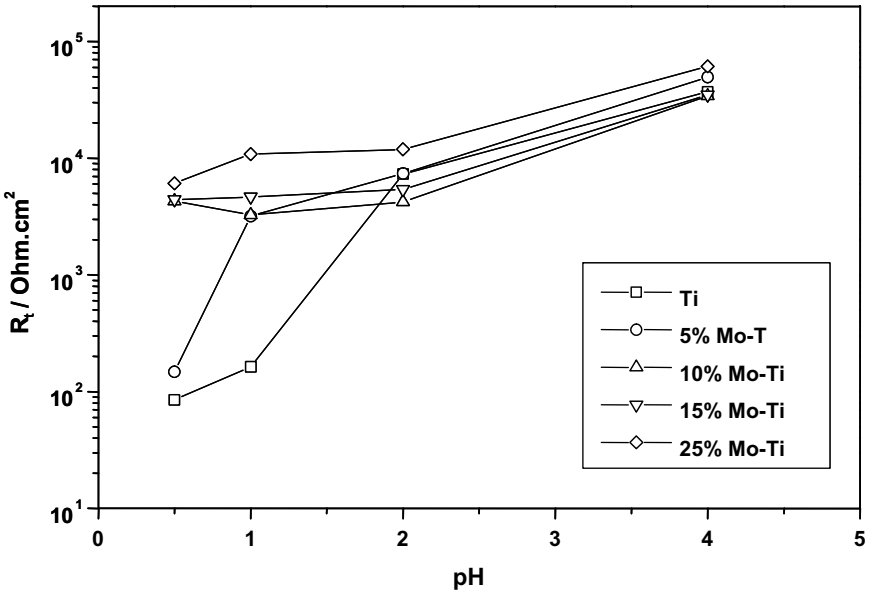

Fig. 8. Plot of Rt values of Ti and Mo–Ti alloys as a function of pH in open circuit potential condition.

capacitance at low frequency was thought to correspond to the double layer capacitance. Ti alloy containing 5% Mo exhibited a similar behavior as evidenced by the very low R_t value of 148 Ω cm^2 at pH 0.5 with two capacitances. However, the 15% Mo–Ti alloy exhibited the very high R_t value of 4400 Ω cm^2 even in the highly acidic condition of pH 0.5. A still higher R_t value of 6100 Ω cm^2 was observed with 25% Mo–Ti alloy. Change of pH of the environment to 1.0 produced a further increase in R_t value of 15% Mo–Ti alloy to 4600 Ω cm^2. This higher R_t value and the absence of a second capacitance peak in the EIS spectra indicated that these alloys were completely dominated by the passive film properties. These results were in good agreement with the results of polarization experiments shown in Fig. 6. In this way, the impedance spectra obtained with Ti and Mo–Ti alloys were depicted by the equivalent circuit as shown in Fig. 9. Here, by adding Mo the equivalent circuit was changed from (a) active to (b) passive condition. Thus, R_t in Fig. 9 corresponded to (a) corrosion reaction resistance (R_{ct}) in the active condition and (b) the film resistance (R_f) in the passivated condition, respectively. Thus, the R_t value at 3 mHz could estimate the corrosion resistance of Ti alloy both in the active and passive conditions. In Fig. 5, pure Ti or 5% Mo-alloy could not keep a high value of R_t at pH 2 and pH 1, respectively. However, R_t of 10–25% Mo-alloy could keep a high value even in low pH solutions.

In order to examine the passive behavior, the specimens were passivated at 500 mV for one hour and impedance spectra were obtained at the same potential. The impedance spectra of Ti and 5–25% Mo–Ti alloys in pH 0.5 solutions are shown in Fig. 10. The plot of R_t values at 3 mHz as a function of % Mo content in Mo–Ti alloys is given in Fig. 11. The passive film capacitances were

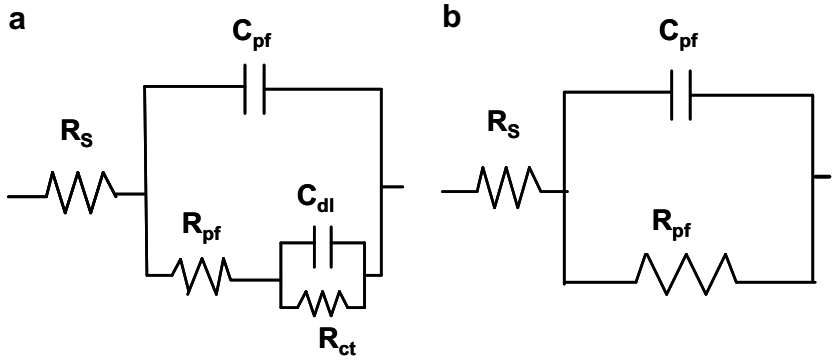

Fig. 9. Equivalent circuits depicting the impedance behaviors of Ti and 5–25% Mo–Ti alloys in pH 0.5 and pH 1.0 solution of 20% NaCl at 100 °C. (a) 0–10% Mo–Ti alloys and (b) 15–25% Mo–Ti alloys (Rs; solution resistance, Rpf; film resistance, Ret: charge transfer resistance, Cpf; film capacitance, Cdl: double layer capacitance).

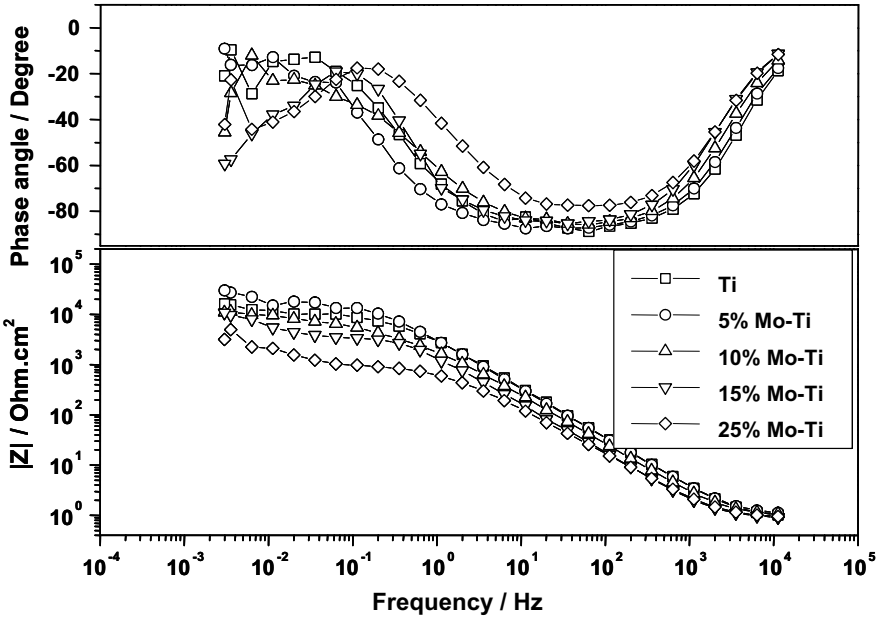

Fig. 10. Impedance behavior of Ti and Mo–Ti alloys in passive region (+500 mV) in pH 0.5 solution of 20% NaCl at l00 °C.

observed for Ti and all alloys, and R_t was as high as 16,000 Ω cm^2 at pH 0.5. The Mo alloys exhibited relatively lower R_t values than pure Ti as is evident from 10,700 and 6160 Ω cm^2 for 15% and 25% Mo–Ti alloys, respectively. However, the R_t values were significantly higher when compared to the corresponding values in the OCP condition. This anomalous behavior in R_t might be attributed to the transpassive dissolution characteristics of Mo through the passive film [18]. Higher Mo content in the alloy was expected to result in higher transpassive dissolution by Mo and thus reduce R_t to lower values. These results corresponded to the increase of the passive current by Mo addition in polarization curves (Fig. 6).

3.5. Breakdown behavior of passive film of Ti and Mo–Ti alloys

It was important to confirm more details about the stability of the passive film on Ti and its alloys for longer durations. Thus, samples were passivated at 500 mV for 1 h, then the open circuit potential (OCP) was measured for 24 h. The potential decays of the samples were monitored as presented in Fig. 12. The OCP of Ti in pH 0.5 solution reached around −700 mV within 20 h. This was almost the same as that observed for the bare metal surface of Ti at the same pH (Fig. 5). Thus, the breakdown of passive film on Ti was found to occur in a short time at pH 0.5. Alloy containing 5% Mo also reached an active corrosion potential value of around −540 mV within 20 h. However, potential decays of 15% and 25% Mo–Ti alloys at this pH were found to be around −260 mV and −220 mV, respectively, even after 24 h, which indicated that stable passive films remained on these alloys even after 24 h.

The impedance spectra of samples passivated at 500 mV for 1 h, then kept at OCP for 10 h, are shown in Fig. 13. The impedance spectra of Ti and 5% Mo–Ti alloy showed two capacitances and very low R_t values, which showed almost the active condition. On the other hand, 10–25% Mo–Ti alloys showed one capacitance and very high R_t values, which showed the passive condition. The plot of R_t values versus Mo content at pH 0.5 and 1.0 are shown in Fig. 14. In pH 0.5 and pH 1.0 environments, R_t values of pure Ti kept for 1 h in the OCP condition after passivation were as low as 130 and 160 Ω cm^2. These were similar to those of the bare metal of Ti shown in Fig. 4. Thus, in the case of Ti, the passive film was broken down completely and active corrosion occurred within a short time even after passivation. The 5% Mo–Ti alloy revealed lower R_t values at around 10 h. In the impedance spectra of Fig. 10, 5% Mo–Ti alloy revealed two capacitances. These behaviors suggested that the oxide film on 5% Mo–Ti alloy was not stable in these environments.

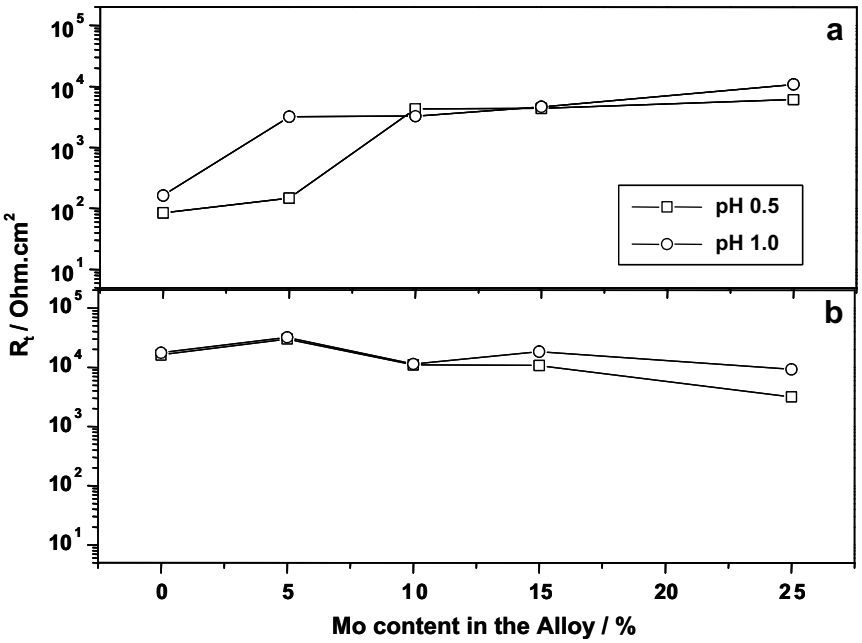

Fig. 11. Plot of Rt values of Ti and Mo–Ti alloys as a function of pH in (a) open circuit condition and (b) passive region.

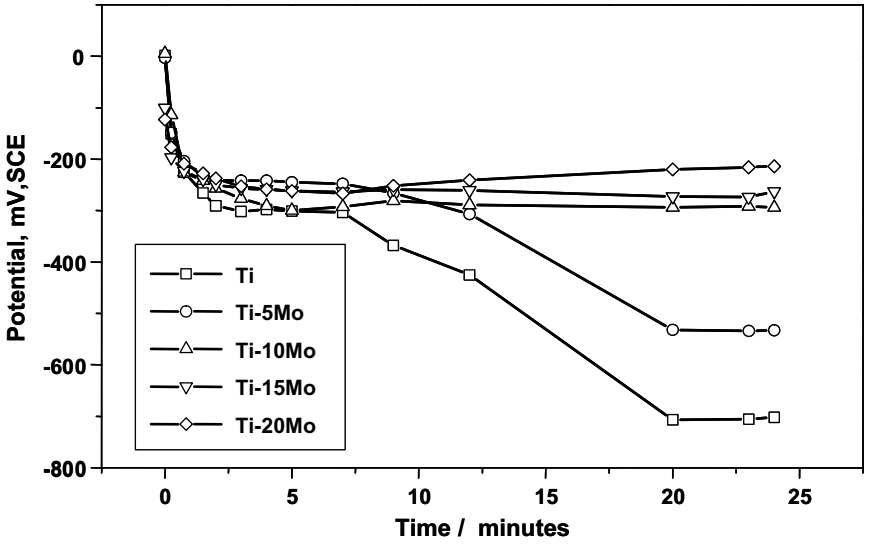

Fig. 12. Open circuit potential decay of Ti–Mo alloys passivated at 500 mV for one hour in pH 0.5 solution of 20% NaCl at 100 °C.

On the contrary, 10–25% Mo–Ti alloys kept higher R_t values throughout the period kept in the OCP condition. For example, the R_t value was around 10,000 Ω cm^2 at pH 0.5 for 24 h. Hence, it was confirmed that the passive films of 10–25% Mo–Ti alloys remained stable in highly acidic chloride solutions at elevated temperature. In this way, adding Mo to Ti alloys conferred very high resistance against crevice corrosion at high temperature.

3.6. Crevice corrosion behavior of Ti and Mo–Ti alloy

In this paper, crevice corrosion of Ti and Mo–Ti alloy was monitored by microelectrodes under the simulated condition for overpacks. In the case of pure Ti, as the concentration of chloride ions increased and pH reduced in the crevice, the crevice current increased. This behavior was explained by the hydrolysis reaction in the crevice, and pure Ti showed susceptibility to crevice corrosion at a temperature of 100 °C. On the other hand, in the case of Mo–Ti alloy, there were few changes in the concentration of chloride ions and pH in the crevice, and little increase in crevice current. From the OCP and polarization measurements, it was revealed that pure Ti could not keep the passive film in the solution of low pH and high chloride concentration. As the hydrolysis reaction in the crevice proceeded, the concentration of chloride ions increased and pH reduced, and the passive film of pure Ti was easily broken down. At 100 °C, the depassivation pH was estimated to be almost 4.0 for the pure Ti in high chloride solution. However, the corrosion potential of Ti alloy was kept in the passive region by the high cathodic current and low anodic peak current caused by the Mo addition. In the case of Mo–Ti alloy, the passive film remained even in the solution of low pH of 0.5 and high chloride concentration. The mechanism of the high corrosion resistance of Pd–Ti alloy can be explained by the stable passive film in acidic

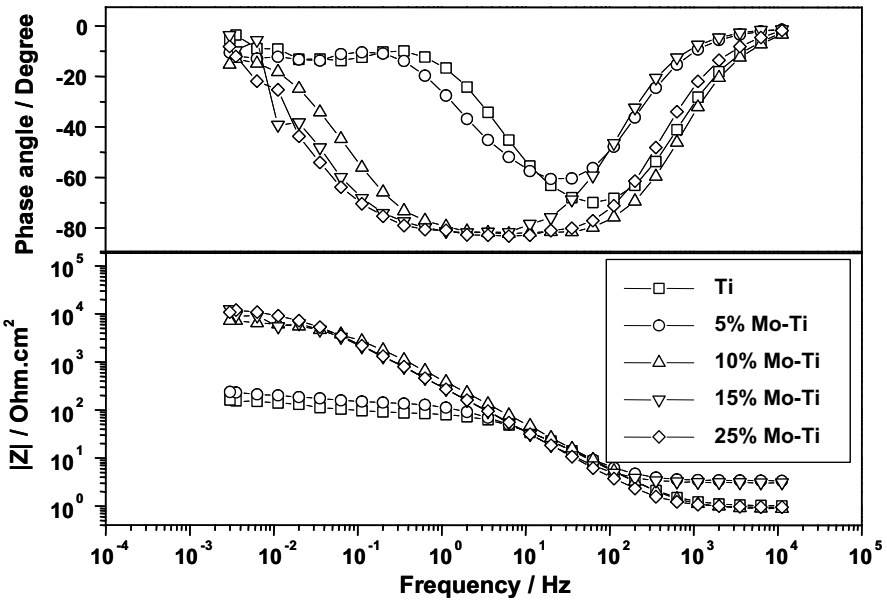

Fig. 13. Impedance behavior of passivated (+ 500 mV) Ti and Mo–Ti alloys kept in OCP for 10 h in pH 0.5 solution of 20% NaCl at 100 °C.

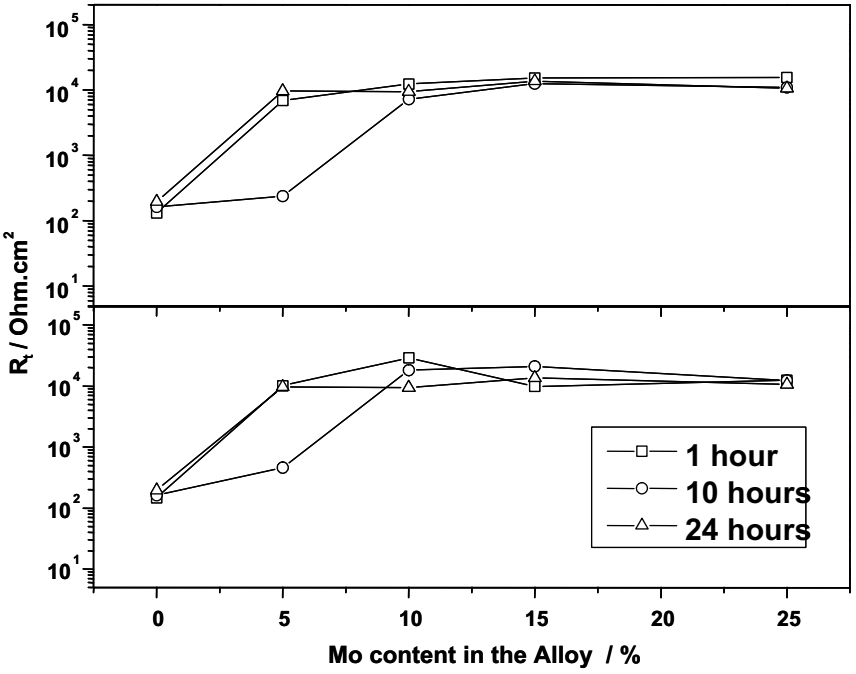

Fig. 14. Plot of Rt values of Ti and Mo–Ti alloys as a function of Mo content after Passivated and kept in open circuit (a). pH 0.5 solution (b) pH 1.0 solution.

solution. Mo–Ti alloy showed almost the same mechanism as that of Pd–Ti alloy. Thus, it may be possible to design high corrosion-resistant Ti alloy without using rare metals.

EIS measurements confirmed the above findings by showing the corrosion resistance, R_t. R_t of pure Ti was a very low value in the low pH solution, and even when the sample was kept in the passive region, R_t immediately changed to a low value because of the breakdown of the films. However, R_t of alloy remained high even in the solution of low pH and high chloride concentration, which showed that the passive film was kept. Thus, Mo–Ti alloy kept the passive film in the simulated crevice solution and showed high resistance against crevice corrosion under environments simulating the overpack near the coast.

4. Conclusions

Crevice corrosion experiments showed that Mo–Ti alloys have higher crevice corrosion resistance in environments with higher chloride concentration. From the crevice corrosion monitoring in 10% NaCl at 100 °C, although a considerably large shift in crevice potential toward the active region and large current were observed with Ti, no change in crevice potential or current was observed with the Mo–Ti alloy. Polarization measurements showed an increase in cathodic current density with the increase of Mo content in Ti alloys. As the Mo content was increased to around 15%, the corrosion potential was found to exist within the passive region even in highly acidic solutions. The higher impedance values

shown by EIS revealed that 15% and 25% Mo–Ti alloys could keep the passive film even in the acidic solutions. Thus, the presence of stable oxide film on the surface of Mo–Ti alloys was responsible for imparting higher resistance to crevice corrosion even in environments of high chloride concentration. It was found that Mo–Ti alloy kept the passive film in such environments at 100 °C. In this way, as for the crevice corrosion, this alloy could be useful for environments simulating the overpack near the coast.

References

[1] John C. Griess Jr., Corrosion 24 (1968) 96.
[2] B. Vicentini, D. Sinigaglia, G. Taccani, Corros. Sci. 15 (1975) 479.
[3] L.A. Yao, F.X. Gan, Y.X. Zhao, C.L. Yao, J.L. Bear, Corrosion 47 (1991) 420.
[4] Xihua He, J.J. Noel, D.W. Shoesmith, J. Electrochem. Soc. 149 (2002) B440.
[5] R.W. Schutz, Corrosion 59 (2003) 1043.
[6] X. He, J.J. Noel, D.W. Shoesmith, Corrosion 60 (2004) 378.
[7] N.D. Tomashov, R.M. Altovsky, G.P. Chernova, J. Electrochem. Soc. 108 (1961) 113.
[8] N.D. Tomashov, G.P. Chernova, Yu.S. Ruscol, G.A. Ayuyan, Electrochim. Acta 19 (1974) 159.
[9] Robert S. Glass, Yang ki Hong, Electrochim. Acta 29 (1984) 1465.
[10] Y.J. Kim, R.A. Oriani, Corrosion 43 (1987) 56.
[11] D.G. Kolmann, J.R. Scully, J. Electrochem. Soc. 140 (1993) 2771.
[12] S.Y. Yu, C.W. Brodrick, M.P. Ryan, S.R. Scully, J. Electrochem. Soc. 146 (1999) 4429.
[13] C.S. Brossia, G.A. Cragnolino, Corrosion 57 (2001) 768.
[14] E. VanderLingen, R.F. Sandenbergh, Corros. Sci. 43 (2001) 577.
[15] C.S. Brossia, G.A. Cragnolino, Corros. Sci. 46 (2004) 1693.